J. Appl. Environ. Biol. Sci., 5(10S)477-489, 2015
© 2015, TextRoad Publication
ISSN: 2090-4274
Journal of Applied Environmental and Biological Sciences
www.textroad.com

Fatigue behavior of geopolymer mortar reinforced by polypropylene fibers under constant loading amplitude and variable block loading

A. Refahi[1], J. Aghazadeh Mohandesi[2], E. Gohari Behjat Abadi[3]

[1]Assistant Professor, Department of Mining, Faculty of Engineering, University of Zanjan.
[2]Professor, Department of Metallurgical Engineering, AmirKabir University of Technology, Tehran, Iran.
[3]MSc student, Department of Metallurgical Engineering, AmirKabir University of Technology, Tehran, Iran.
Received: April 20, 2015
Accepted: June 15, 2015

ABSTRACT

Fatigue behavior of geopolymer mortar reinforced by polypropylene fibers under constant loading amplitude and variable block loading has been studied here; the geopolymer source material was Metakaolin prepared by calcining Kaolin powder at 750° C. A fatigue-three-point-bending test was carried out on the geopolymer matrix, plain and reinforced geopolymer mortar in order to examine growth of crack length generated after one loading cycle. The obtained results showed that the fibers not only enhanced fatigue life of the reinforced specimens but also decreased growth rate of fatigue crack length and damage rate. In addition, the fibers increased final crack length prior to fracture. The results acquired from variable block loading test illustrated that under variable block loading, the strength of the studied mortar was remarkably sensitive to kinds of loading; fatigue life of specimens under descending amplitude was decreased in comparison by those under ascending, descending-ascending and ascending-descending amplitude. Finally, fatigue life of the mortar specimens under variable block loading was calculated using the damage curve approach; the estimated results were almost close to data experimentally evaluated.
KEYWORDS: Geopolymer mortar; Fatigue behavior; Variable block loading; Damage.

1. INTRODUCTION

It seems that geopolymer mortar may have remarkable mechanical properties with reasonable price to be considered as a new and environment friendly construction material. Alkali-activated materials called geopolymer, one of the three-dimensional aluminosilicate minerals with semicrystalline to noncrystalline structures introduced in early 1990s, exhibit similar mechanical behavior to that of conventional Portland cements. Geopolymer is produced through chemical reactions between a highly reactive aluminosilicate source and an alkaline solution, and the hardened gel products formed by this reaction process can present desirable mechanical performance in many applications. Its source can be some industrial aluminosilicate waste materials (Xu and Van Deventer, 2000; Davidovits, 1991). The production of geopolymeric cement requires much lower calcining temperature (600–800° C) and emits 80–90% less CO_2 than Portland cement. Reasonable strength can be gained in a short period at room temperature. In most cases, 70% of the final compressive strength is developed in the first 12 hours. Low permeability, comparable to natural granite, is another property of geopolymeric cement. It is also reported that resistance to fire and acid attacks for geopolymeric cement are substantially superior to those for Portland cement. Apart from the high early strength, low permeability and good fire and acid resistance, geopolymeric cement also can attain higher unconfined compressive strength and shrink much less than Portland cement. Other documented properties include good resistance to freeze–thaw cycles as well as excellent solidification of heavy metal ions. These properties make geopolymeric cement a strong candidate for substituting Portland cement applied in the fields of civil, bridge, pavement, hydraulic, underground and military engineering (Davidovits, 1991; Barbosa and MacKenzie, 2003; Papakonstantinou et al., 2001; Singh et al., 2004; Yunsheng et al., 2008). However, the poor mechanical properties of geopolymer materials usually result in catastrophic failure during service, which is a well-known impediment to their wide applications (Zhao et al., 2007). Some short fibers, such as polyvinyl alcohol (PVA), polypropylene (PP), basalt fibers and carbon fiber, were employed as additives to improve geopolymeric mechanical performance because fibers were capable of providing a control of cracking and increasing the fracture toughness of the brittle matrix through bridging action during both micro and macro cracking of the matrix (Zhang et al., 2010). For example, it was reported that short polyvinyl alcohol (PVA) fibers were used to reinforcing fly ash/Metakaolin-based geopolymer and no crack was found on the surface of geopolymer paste with 2% of PVA fiber (Zhang et al., 2006). The short PVA fibers with an optimum volume fraction of 1% were successfully employed to improve the brittle properties of ash-based geopolymer (Sun and Wu, 2008). Zhang et al. reported that calcined kaolin/fly ash-based geopolymer reinforced by polypropylene (PP) fibers showed increasing compressive and flexural strengths when the geopolymer was cured in steam at 80° C for 3 days (Zhang et al., 2009). Dias and

Corresponding author: A. Refahi, Assistant Professor, Department of Mining, Faculty of Engineering, University of Zanjan. Postal address: Assistant Professor, Department of Mining, Faculty of Engineering, University of Zanjan, Tabriz Road, Zanjan, Iran. Postal code: 45371-38791 Tel Number: +989123034360 E-mail address: refahi.arash@znu.ac.ir; refahi.arash@gmail.com

Thaumaturgo investigated fracture toughness of geopolymeric concretes reinforced with basalt fibers. It was found that the geopolymeric concretes with volume fractions of 0.5–1% basalt fibers showed higher splitting tensile strengths than that of Portland cement concretes (Dias and Thaumaturgo, 2005). Li and Xu reported that the addition of basalt fiber with an optimum volume fraction of 0.3% could significantly improve deformation and energy absorption capacities of geopolymeric concrete (Li and Xu, 2009). Lin et al. stated that the short carbon fibers were used to increasing the flexural strength and toughness of geopolymer (Lin et al., 2008, 2010). Natali et al. showed that glass fiber reinforced geopolymer composites exhibited a flexural strength increment from 30% up to 70% and geopolymer composites containing PVC and carbon fibers exhibited the best energy absorption capacity (Natali et al., 2011).

In this study, fatigue behavior of the geopolymer matrix and geopolymer mortar (made by mixing geopolymer and silica sand particles) and the reinforced mortar by short polypropylene fibers was studied. For this purpose, a three point bending test was initially carried out on the studied specimens, and subsequently a bending fatigue test was performed with constant loading amplitude and variable block loading (i.e. ascending, descending, ascending-descending and descending-ascending loading amplitude). During these tests, bending strength, fatigue life, crack growth rate and damage growth rate of the studied specimens were determined. In addition, the curves of damage rate during the fatigue test were determined and used to predict the fatigue life of geopolymeric mortar under the variable block loadings.

2. MATERIALS AND METHODS

In this work, the geopolymer matrix was produced by mixing Metakaolin, sodium hydroxide, sodium silicate and water with weight ratio of 53%, 4.2%, 34% and 8.8%, respectively. Metakaolin was prepared by calcining Kaolin powder at 750° C for 3 hours to obtain an amorphous structure that was examined by XRD (X-Ray Diffraction), FTIR (Fourier Transform Infrared Spectroscopy) analysis; chemical composition and physical properties of Metakaolin are given in Table 1 and 2. Sodium hydroxide solution was produced by mixing water and sodium hydroxide powder, and then sodium silicate was added in order to make an activator solution; the mixture was stirred until a transparent solution was acquired (Table 2 and 3). This activator was gradually and continually poured on the Metakaolin powder and the obtained gel (i.e. geopolymer) was stirred for 5 minutes. In order to produce geopolymer mortar, sand particles with different weight ratios (i.e. 10, 20, 30, 40, 50, 60%) were added to the geopolymer gel and the mixture was stirred for 5 minutes and poured into the rectangular cube molds with 350*100*100 mm dimensions based on ASTM-1018-94b standard as shown in Fig. 1; the molds were produced from polyethylene sheets with 10 mm thickness. The XRD analysis followed by chemical analysis showed that the composition of sand particles is pure silicon dioxide (99%). The size distribution and physical properties of sand particles is shown in Table 4. For the purpose of polypropylene fiber reinforced mortar, monofilament fibers shown in Fig. 2a with 12 mm length and 0.3 mm thickness were manually fibrillated (Fig. 2b); the properties of polypropylene are given in Table 5. Then the fibers with different volume ratios (i.e. 2, 3 and 5%) were added to the mortar gel and the mixture was stirred to obtain a homogeneous morphology. It has been shown that the fiber with 12 mm length and 1-5% volume fraction has the best performance for reinforcing geopolymer concretes (Akkaya et al., 2000; Gonzalez and Lorca, 2006). Finally, the reinforced gel was poured into the molds. The molds remained in the room temperature for 3 hours to complete the polymerization process, and then the specimens were located in an oven with 65° C for duration of 48 hours.

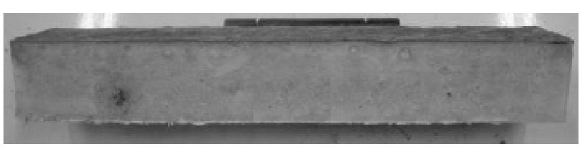

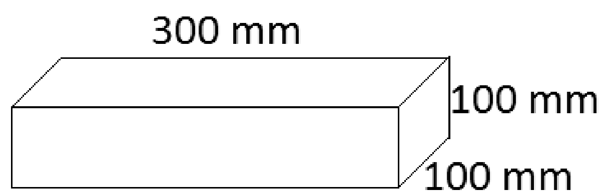

Fig. 1. A rectangular cube specimen of geopolymer mortar.

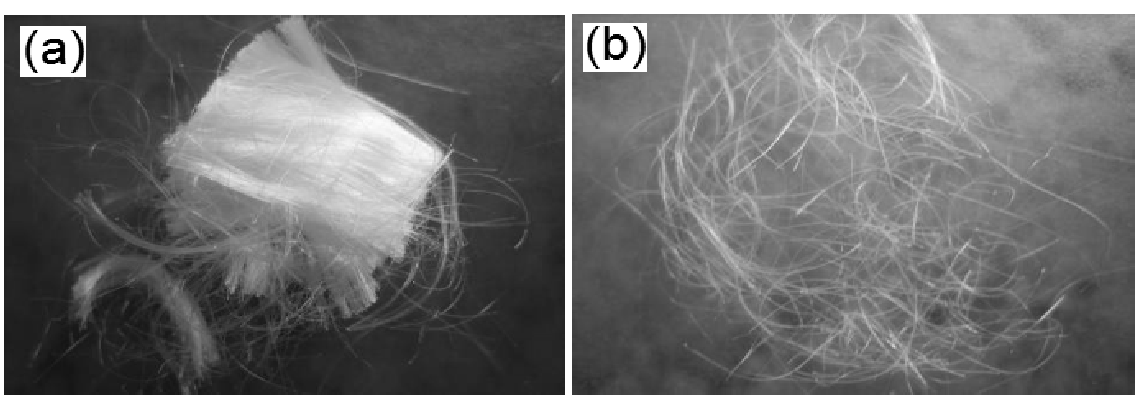

Fig. 2. (a) Monofilament and (b) fibrillated polypropylene fibers.

Mineral	weight ratio %
SiO_2	64
Al_2O_3	23
Fe_2O_3	0.65
TiO_2	0.04
Cao	11.31
MgO	0.35
Na_2O	0.4
K_2O	0.25

Table 1. Chemical composition of Metakaolin.

Physical property	Metakaolin	Sodium silicate	Sodium hydroxide
Specific gravity	3.51	2.4	2.13
Bulk density	830	513	961
Molar mass g/mol	222.1	122.1	40

Table 2. Physical properties of Metakaolin, sodium silicate and sodium hydroxide powder.

Mineral	Weight ratio %
Na_2O	7
SiO_2	30.5
H_2O	62.5
Specific gravity of sodium silicate solution	1.39

Table 3. Chemical composition of sodium silicate solution.

Size mm	Weight fraction passing %	
2.36	85.3	
1.7	65.8	
1.4	38.5	
0.85	5.7	
Physical properties of sand particles	Density Kg/m^3	2600
	Elastic modulus GPa	72
	Uniaxial compressive strength MPa	160

Table 4. Size distribution and properties of silica sand particles.

Property	Value
Density Kg/m^3	910
Elastic modulus GPa	8.5
Tensile strength MPa	580
Melting point $°C$	160

Table 5. Properties of polypropylene fibers.

To determine the optimum value of sand particle weight fraction and polypropylene fiber volume fraction, ten samples of each specimen were employed for a bending test using a servo hydraulic Instron testing machine (Instron 8502); Fig. 3 illustrates a geopolymer mortar specimen is loaded by the machine. The specimens were located on two-roller supports with 25 cm apart and the force was applied by a rigid cylinder with 10 mm in diameter acting on the middle part of the specimen under the displacement rate of 0.5 mm/min until the first crack appears in the studied mortar. To obtain the accurate results, the surface of the specimens was constantly monitored during the experiment by stopping the test and accurate examination using dye penetrant technique. The plain mortar with optimum value of sand particles was determined first, and subsequently the reinforced mortar with optimum value of fibers was investigated.

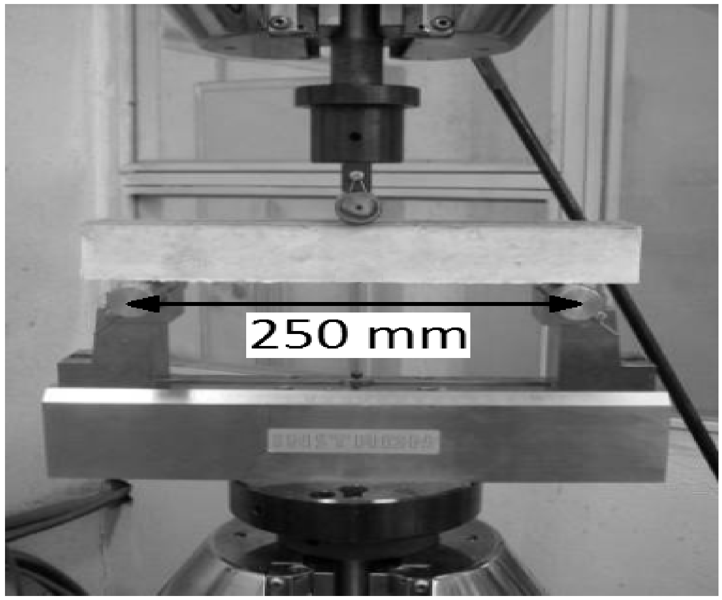

Fig. 3. Three point bending test applied to a geopolymer mortar specimen.

In order to determine the fatigue life of geopolymer mortar, a standard fatigue bending test was carried out on ten samples of each studied specimen using the Instron universal testing machine (Fig. 3); the dimension of the fatigue specimens was similar to that of the three point bending test. The frequency of cyclic loading was 1 Hz in the sinusoidal waveform. The maximum applied load was 70%, 80% and 90% of the fracture load in the static bending test. To insure the contact between the specimens and the jaws of the machine test, a minimum load of 0.1 KN was applied. In order to obtain the fatigue crack growth rate, the generated crack after one loading cycle was taken as the initial crack length, and then the growth of crack length during the test was examined using a special designed microscope. Also, to determine the fatigue life under variable block loading amplitude, repeating an unit loading block of ascending, descending, ascending-descending and descending-ascending (Fig. 4) were applied to the ten specimens of each studied mortar until fracture.

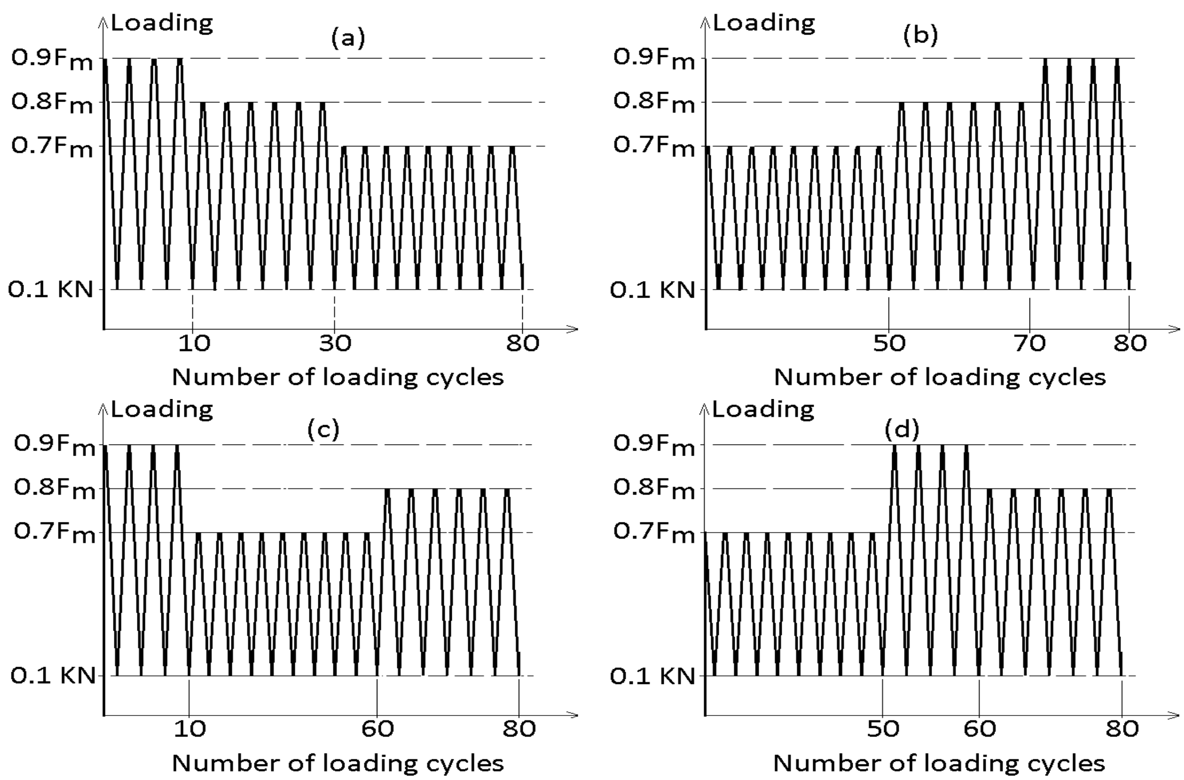

Fig. 4. An unit loading block: a) descending, b) ascending, c) descending-ascending, d) ascending-descending (F_m is fracture load in the static bending test).

3. RESULTS AND DISCUSSION

3.1. Bending test

Table 6 shows the results obtained from the static-bending test applied to the specimens of geopolymer matrix; the scatter of obtained fracture load is remarkably high. This is common for geopolymer matrixes under three point bending test where the flaws vary in size, shape and orientation, causing the fracture load to vary from specimen to specimen (Meyers and Chawla, 2009). Weibull statistical approach was used to determine the statistically most probable results. The basic assumption in Weibull distribution is that a body of a material has a statistical distribution of noninteracting fractures. If there are N broken specimens of a brittle material that were tested, the fracture probability of a specimen with number of i ($F_i(V)$) is equal to:

$$F_i(V) = i/(N+1) \tag{1}$$

Based on Weibull distribution, the fracture probability of each specimen can be related to the maximum applied load or fracture load (F) as follow:

$$1 - F(V) = \exp\left[(F/F_0)^m\right] \tag{2}$$

Where F_0 is a characteristic fracture load of the material that it is often defined as the mean fracture load, and m is the Weibull modulus measuring the variability of the obtained data; the higher the value of m, the less is the material variability in fracture load. A double-logarithmic plot of Eq(2) will give a straight line with slope m as following expressed (Meyers and Chawla, 2009):

$$\ln\left[\ln\left(1/(1-F(V))\right)\right] = m\ln F - m\ln F_0 \tag{3}$$

Consequently, the mean fracture load and the corresponding Weibull modulus can be evaluated by passing the best line through the points given in Table 6 using the regression approach (Kreyszig, 2006). Similar approach was employed for results obtained by applying the test to other studied specimens, and the mean fracture loads of them were determined. Fig. 5 shows the variation of mean fracture load of the plain geopolymer mortar with the different amount of sand particles. The specimen with 30% sand particles has the highest fracture load (1.35 KN); by increasing the weight percent of particles up to 30%, the fracture load of mortar increases and beyond that (i.e. 40%, 50% and 60% sand) it decreases. It seems that by increasing the amount of sand up to 60% the strength of mortar decreases due to over population of particles, causing poorly bonds to occur between them (Aghazadeh et al., 2011). Fig. 6 illustrates the mean fracture load of the reinforced geopolymer mortar with 30% sand versus the different values of fiber volume fraction. It seems that the reinforced mortar with 2% fiber has the highest strength (7.2 KN); by increasing the fibers up to 2%, the fracture load of mortar increases and beyond that (i.e. 3% and 5% fibers) it decreases.

The geopolymer mortar samples carry flaws and micro cracks both in the material and at the interfaces. Under an applied load, the distributed micro cracks propagate, coalesce and align themselves to produce macro cracks. When load are further increased, conditions of critical crack growth are attained at the tips of macro cracks and a catastrophic failure is precipitated. However, the fibers bridge the propagating cracks in the reinforced specimens because the matrix failure precedes the fiber failure. This causes the fiber bridging zone to absorb a lot of energy by fiber debonding, fiber pullout (sliding) and fiber rupture when a crack propagates across a fiber through the matrix as illustrated in Fig. 7. Consequently, the fibers enhance the energy absorption capacity and reduce the cracking sensitivity of the mortar, causing the fracture strength to increase (Banthia and Sheng, 1996). In addition, the fibers reduce the shrinkage contraction and thus reduce the interfacial relative slides between the matrix and other additive materials, causing to improve the interfacial bonding strength (Sun and Xu, 2009).

Number of specimen	Fracture probability $F(V)$	Fracture load KN
1	0.091	2
2	0.182	1.66
3	0.273	1.4
4	0.364	1.63
5	0.455	1.48
6	0.545	1.7
7	0.636	2.1
8	0.727	1.57
9	0.818	1.45
10	0.909	1.51

Table 6. Fracture load of ten specimens of geopolymer matrix.

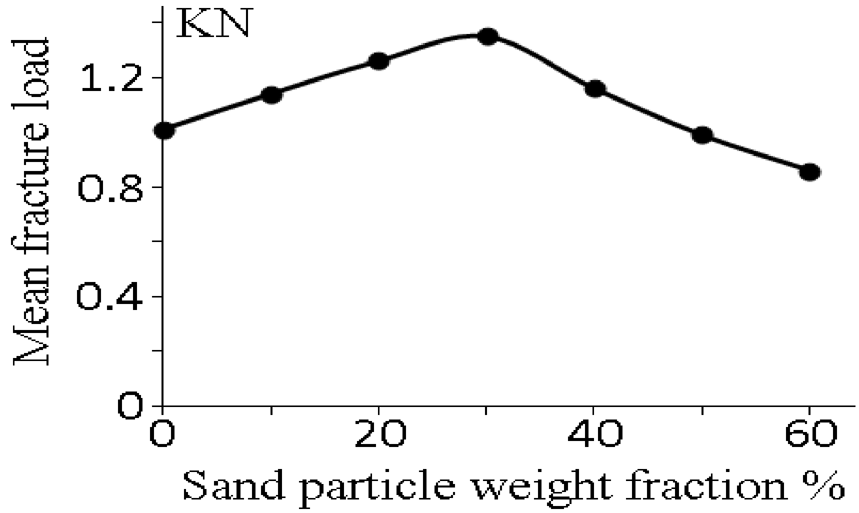

Fig. 5. Mean fracture load of plain geopolymer mortar versus different sand particle weight fractions

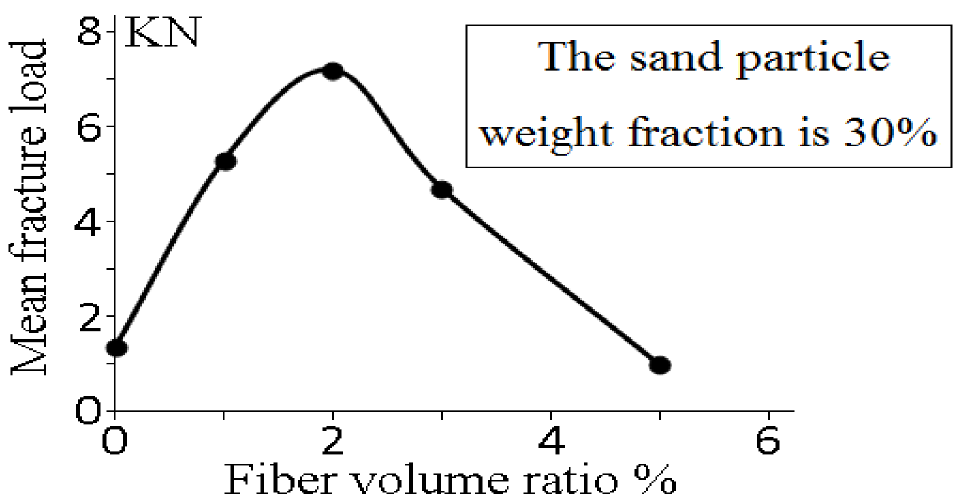

Fig. 6. Mean fracture load of reinforced geopolymer mortar with 30% sand versus different fiber volume fractions.

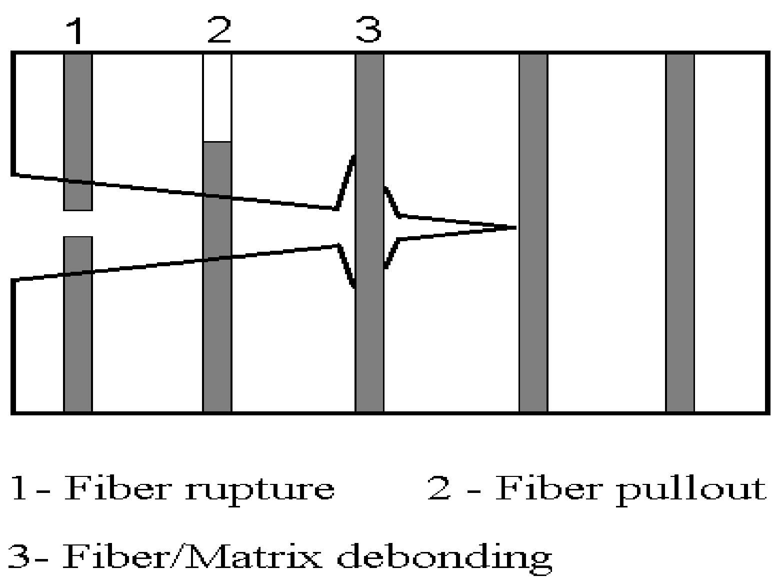

Fig. 7. Methods of absorbing energy in fiber bridging zone.

3.2. Fatigue test with constant loading amplitude

Similar to the static-bending test, the mean value of fatigue life, initial crack length and final crack length prior to fracture of the plain mortar with 30% sand particles and reinforced mortar by 2% polypropylene fibers was determined and given in Table 7; these results indicated that the polypropylene fibers remarkably increased the fatigue life of the reinforced specimens. In addition, the crack growth rate during the fatigue test is shown in Fig. 8, 9 and 10. The obtained results showed that the retarding effect of fibers on the crack growth rate. The ultimate crack length prior to final fracture of the reinforced mortar was greater than that of the plain mortar under the applied maximum load of $0.9F_m$ and $0.8F_m$ (F_m was the mean fracture load in the static-bending test). However, at $0.7F_m$ this difference diminished (Fig. 8, 9 and 10).

Maximum Load KN		Mean initial crack length cm (a_0)	Last recorded cycle at that final crack length was measured (N_f)	Mean final crack length cm (a_f)	Mean fatigue life
Plain geopolymer mortar	0.95	0.42	1350	4.5	1383
	1	0.53	480	3.7	492
	1.2	0.8	90	3.3	93
Reinforced geopolymer mortar	5	0.35	2900	4.6	2941
	5.8	0.4	1750	4.2	1775
	6.5	0.58	400	3.8	411

Table 7. Results evaluated from fatigue bending test with constant loading amplitude.

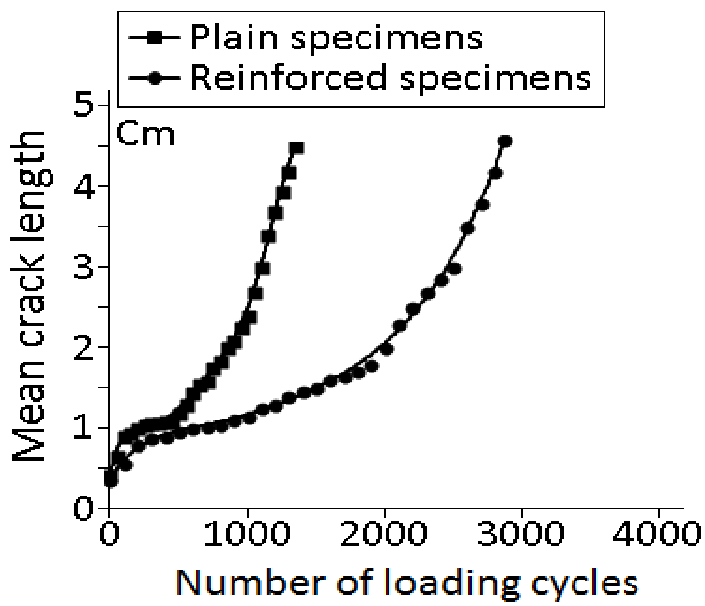

Fig. 8. Crack growth rate in the geopolymer mortar (maximum applied load is $0.7F_m$).

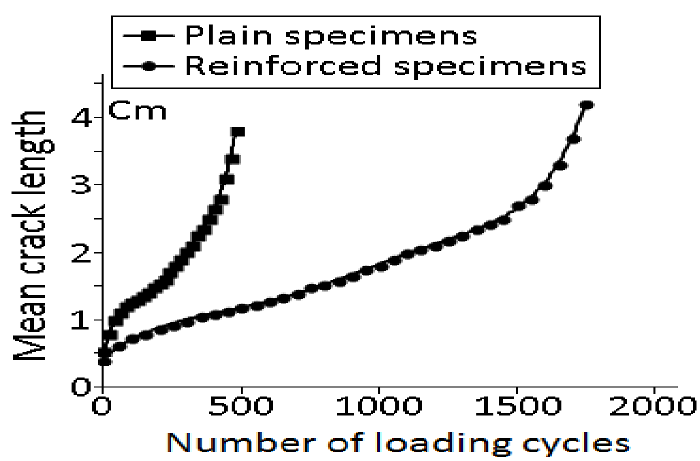

Fig. 9. Crack growth rate in the geopolymer mortar (maximum applied load is $0.8F_m$).

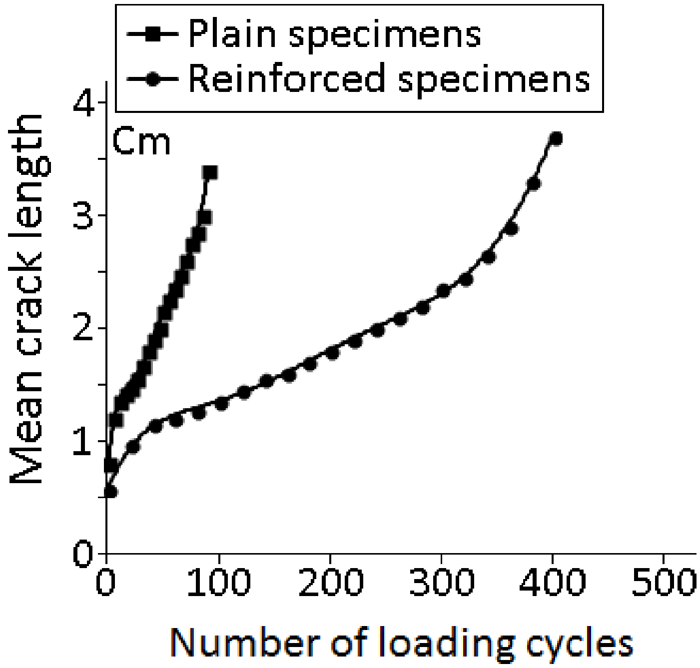

Fig. 10. Crack growth rate in the geopolymer mortar (maximum applied load is $0.9F_m$).

In order to estimate the damage accumulated in the studied mortar, the damage curve theory was used; the damage after applying n loading cycles is equal to (Manson and Halford, 1981):

$$D = a / a_f \tag{4}$$

Where D is the damage, a is the crack length formed in the specimens after applying n loading cycles, and a_f is the ultimate crack length (Table 7); when the damage is equal to 1, the specimen will be broken. The damage versus the relative loading cycles (n / N_f, Table 7) were determined and shown in Fig. 11, 12 and 13; subsequently the best curve passing through these points were obtained using the regression approach (Table 8); The regression equations given in Table 8 will be used for predicting the fatigue life of mortar under variable block loading. The results showed that the difference between damage growth rate in the plain and reinforced geopolymer mortar under low loading (i.e. $0.7F_m$) was not significant. However, the damage growth rate in the plain mortar was greater than that in the reinforced mortar under high loading (i.e. $0.8F_m$ and $0.9F_m$); by increasing the amount of loading, this difference increased. It seems that under low cyclic loading the effect of fibers on crack growths is less significant than that under high cyclic loading.

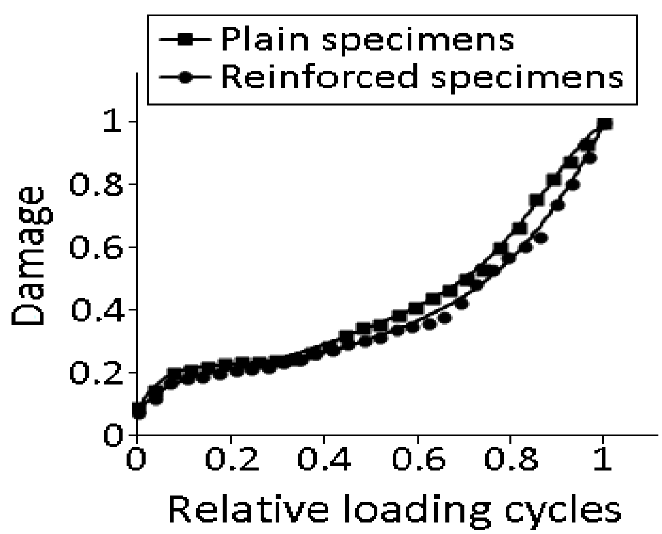

Fig. 11. Damage growth rate in the geopolymer mortar (maximum applied load is $0.7F_m$).

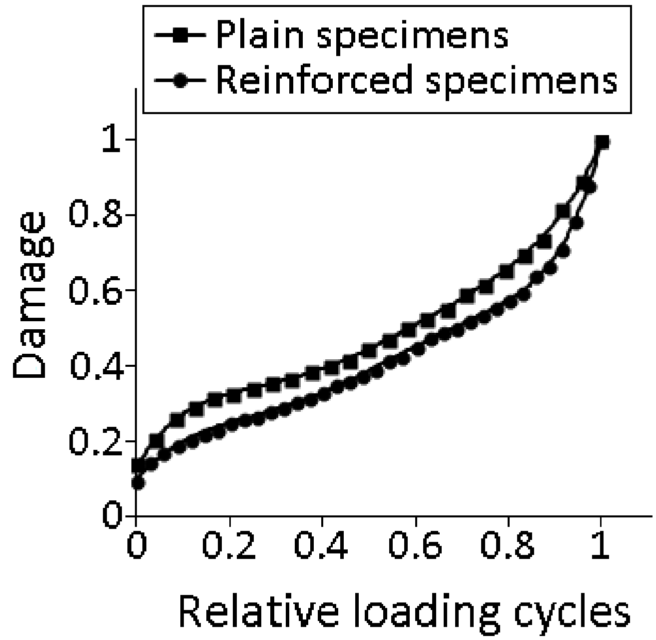

Fig. 12. Damage growth rate in the geopolymer mortar (maximum applied load is $0.8F_m$).

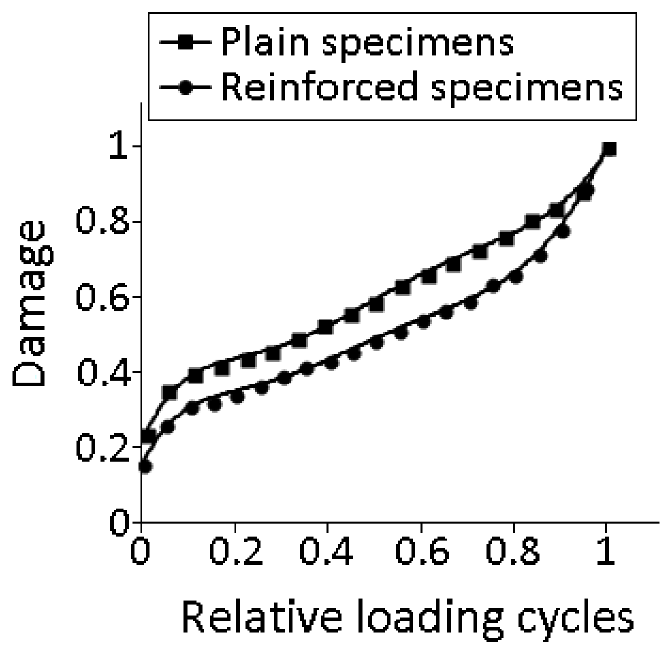

Fig. 13. Damage growth rate in the geopolymer mortar (maximum applied load is $0.9F_m$).

Maximum Load KN		$D = f(n/N_f)$	R^2
Plain geopolymer mortar	0.95	$D = -35.031(n/N_f)^6 + 106.58(n/N_f)^5 - 124.37(n/N_f)^4 + 70.711(n/N_f)^3 - 19.623(n/N_f)^2 + 2.6417(n/N_f) + 0.0838$	0.9988
	1	$D = 0.7185(n/N_f)^6 + 6.8523(n/N_f)^5 - 20.393(n/N_f)^4 + 20.724(n/N_f)^3 - 9.1532(n/N_f)^2 + 2.1191(n/N_f) + 0.1344$	0.9997
	1.2	$D = -10.614(n/N_f)^6 + 44.013(n/N_f)^5 - 67.174(n/N_f)^4 + 48.092(n/N_f)^3 - 16.505(n/N_f)^2 + 2.9661(n/N_f) + 0.2138$	0.9978
Reinforced geopolymer mortar	5	$D = -8.8282(n/N_f)^6 + 30.655(n/N_f)^5 - 40.372(n/N_f)^4 + 26.831(n/N_f)^3 - 9.0652(n/N_f)^2 + 1.6965(n/N_f) + 0.0768$	0.9977
	5.8	$D = 11.065(n/N_f)^6 - 20.303(n/N_f)^5 + 7.8723(n/N_f)^4 + 5.1704(n/N_f)^3 - 4.2551(n/N_f)^2 + 1.3455(n/N_f) + 0.103$	0.9995
	6.5	$D = -15.127(n/N_f)^6 + 54.688(n/N_f)^5 - 73.914(n/N_f)^4 + 47.874(n/N_f)^3 - 15.204(n/N_f)^2 + 2.6199(n/N_f) + 0.155$	0.9992

Table 8. Relation between damage (D) accumulated in the studied mortar and relative loading cycles (n/N_f) determined from regression approach (R^2 is correlation factor (Kreyszig, 2006))).

3.3. Fatigue test with variable block loading

Similarly, the mean fatigue life of the studied geopolymer mortar under variable block loading was evaluated and given in Table 9; it seems that the strength of geopolymer mortar is intensively sensitive to kind of loading amplitude. The fatigue life of plain and reinforced specimens under the descending amplitude was remarkably decreased in comparison by those under the ascending, descending-ascending and ascending-descending amplitudes where not a meaning difference was observed among those. It showed that on descending regime the initial high load amplitudes would result in numerous cracks that can grow on the subsequent low amplitude loading, whereas on the ascending regime the initial loading cycles would merely have any effect on crack formation.

Block loading	Mean number of unit loading blocks applied to failure		Fatigue life	
	Plain mortar	**Reinforced mortar**	**Plain mortar**	**Reinforced mortar**
Ascending	6	20	6*80 = 480	20*80 = 1600
Descending	3	16	3*80 = 240	16*80 = 1280
Ascending-Descending	6	20	6*80 = 480	20*80 = 1600
Descending-Ascending	5	19	5*80 = 400	19*80 = 1520

Table 9. Mean fatigue life of the studied geopolymer mortar under variable block loading.

In order to estimate the fatigue life under the variable block loading, the determined curves of damage growth versus the relative loading cycle has been used. Fig. 14 shows the process of estimating the fatigue life of the plain geopolymer mortar under the descending amplitude; when initially 10 loading cycles with the maximum load of 1.2 KN is applied to the mortar, the damage will be equal to 0.396 (curve No. 1, $n = 10$). Subsequently the maximum load decreases to 1 KN, where the required cycles under this loading amplitude to cause similar damage of 0.396 is equal to 194 (curve No. 2). Consequently, when 20 cycles of 1 KN load is applied to the specimen, the damage will be equal to 0.417 (now curve No. 2, $n = 194 + 20 = 214$). Subsequently the maximum load decreases to 0.95 KN (i.e. 815 loading cycles is required to occur the damage of 0.417, curve No. 3) and 50 cycles are applied to the specimens, causing a damage of 0.445 (curve No. 3, $n = 815 + 50 = 865$). When the specimen breaks, the damage will be equal to 1. Therefore, this loading block must be repeated until fracture (D = 1). The similar treatment has been applied for the plain and reinforced mortar under other loading programs. The obtained results were shown in Table 10; it indicates that the damage curve approach might be a suitable method for approximately predicting the fatigue life of the plain and reinforced geopolymer mortar under the variable block loading amplitudes.

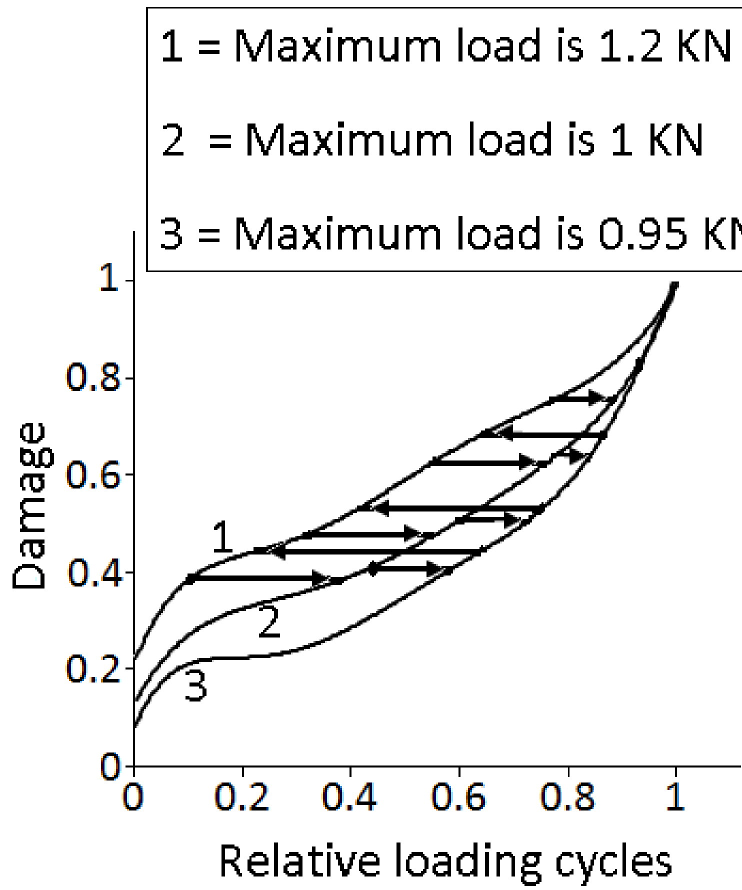

Fig. 14. Process of estimating damage accumulated in the plain geopolymer mortar under variable block loading with descending amplitudes.

Block loading	**Number of block loading applied to specimen prior fracture**			
	Plain mortar		Reinforced mortar	
	From experimental tests	From damage curves	From experimental tests	From damage curves
Ascending	6	5	20	18
Descending	3	4	16	14
Ascending-Descending	6	6	20	17
Descending-Ascending	5	4	19	17

Table 10. Fatigue life of the studied geopolymer mortar under variable block loading determined from the experimental tests and damage curves.

4. Fractographic examination

In order to investigate the fatigue fracture mechanism, fractographic examinations were carried out on the fracture surface of the studied mortar as shown in Fig. 15 and 16; the fiber bridging zone is shown in Fig. 15b. Low flexural displacement was observed in the plain specimen, illustrating that a catastrophic fracture has occurred in the plain geopolymer mortar (Fig. 15a) unlike that of the reinforced specimen where exhibited a typical progressive fracture behavior rather than a catastrophic one (Fig. 15b). These results have been obtained in the previous work [16]. Also, the multiple cracks were observed in the reinforced mortar, causing thin layers of the specimen to be separated from the lateral specimen surface. This may be due to the separation of surface layer of the specimen from the reinforced fibers during the bridging mechanism (Fig. 15b and 6).

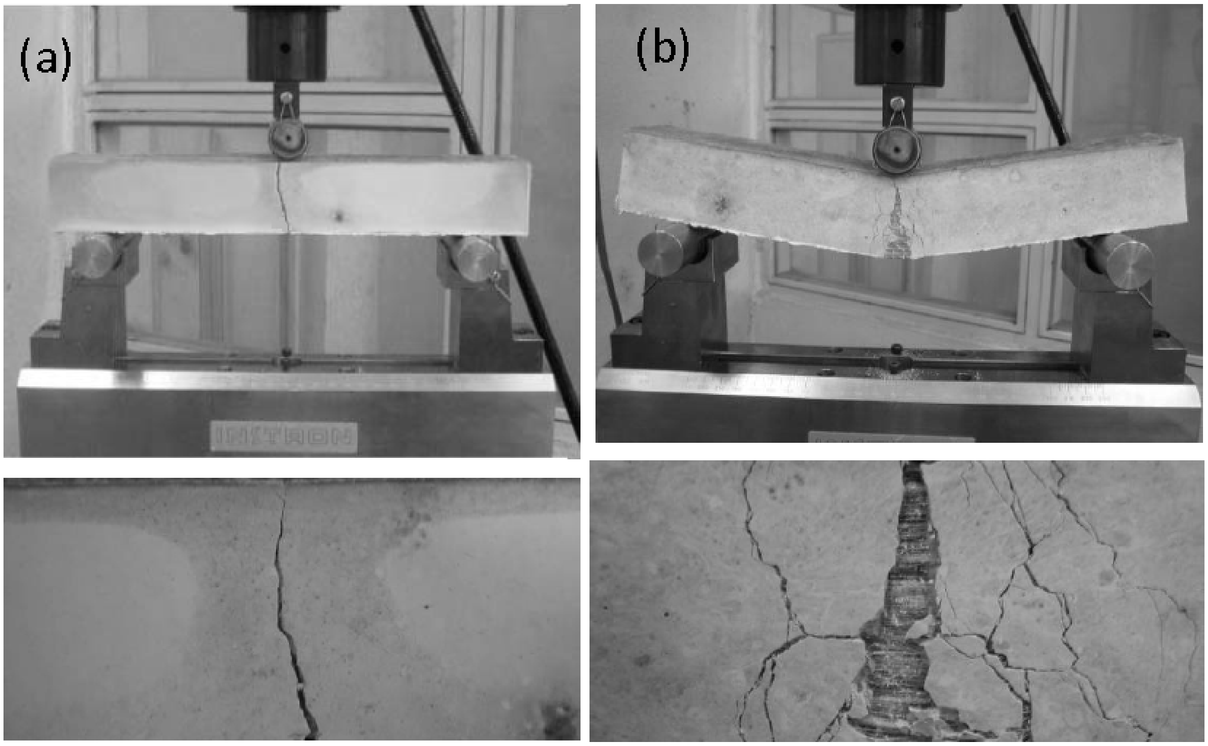

Fig. 15. Fracture mechanism of a) a plain and b) a fiber reinforced geopolymer mortar.

Fracture surface of the fiber reinforced specimens was also examined by Philips XL20 scanning electronic microscope (SEM) as shown in Fig. 16. It seems that the fiber deformation (i.e. thinning and stretching due to fiber rupture) is not considerable, and no damage was observed at the fiber surface (Fig. 16b and 16c). Also, no sight of the fiber/matrix debonding was observed on the fracture surface (Fig. 16c). Some geopolymer particles were seen on the surface of fibers as shown in Fig. 16d. This observation reveals that the dominant micro fracture mechanism is pull out of polypropylene fibers from the geopolymer matrix as shown in the previous study using fibers with the embedded length 38 mm (Singh et al., 2004). It has been suggested that the adhesion and wettability of the polymeric fibers to the cementitious matrix were poor as a result of their chemical inertness and low surface energy, resulting in a weak bond with the cement matrix (Wu, 1982). Considering the shorter length of the polypropylene fibers (i.e. 12 mm) in the present study, the energy absorption mechanism in the reinforced specimens is more likely to be pullout rather than the other mechanisms such as rupture and debonding.

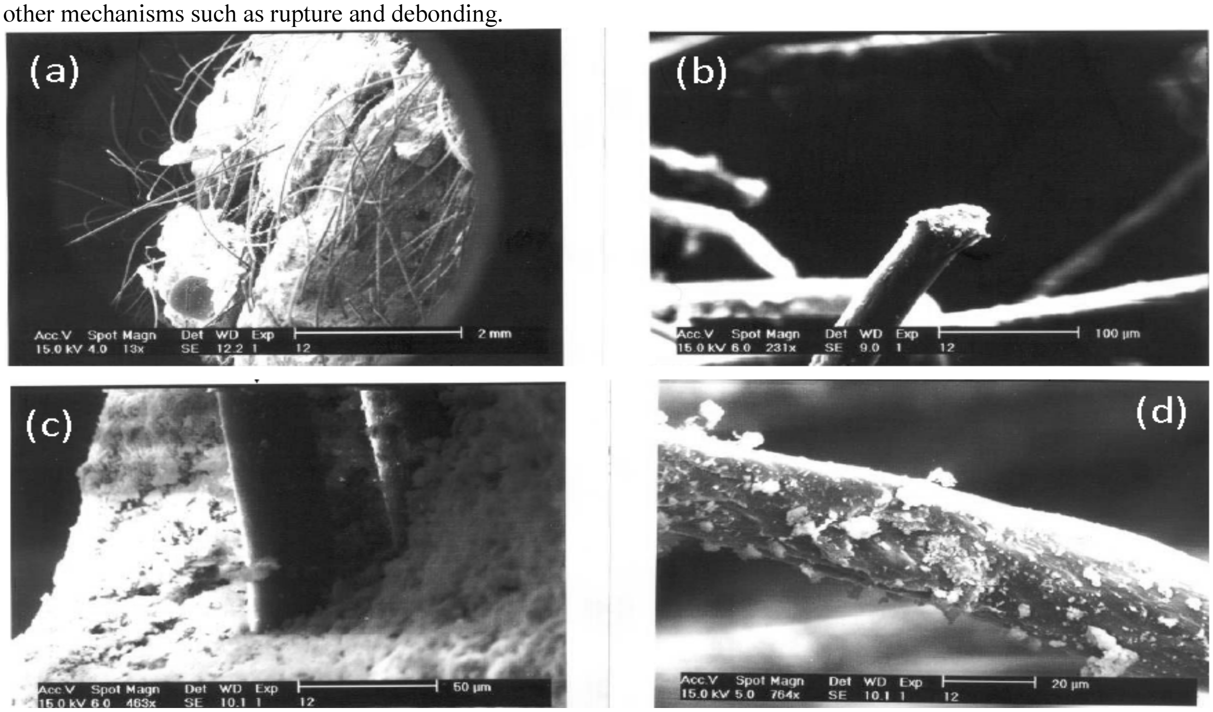

Fig. 16. Scanning electron photomicrograph of fracture surface of a reinforced geopolymer mortar.

5. Conclusion

Experimental investigations were carried out to evaluate the fatigue-bending behavior of the plain geopolymer mortar and the geopolymer mortar reinforced by short polypropylene fibers. Based on the obtained results, the following conclusions have been drawn:

- The polypropylene fibers remarkably enhanced the bending strength of the reinforced mortar. Also, the fibers increased the fatigue life of reinforced specimens under the constant loading amplitude and variable block loading.
- The retarding effect of fibers on the crack growth rate has been determined. The ultimate crack length prior to final fracture of the reinforced mortar was greater than that of the plain mortar under the high cyclic loading (i.e. 0.8 and 0.9 of the mean fracture load in the static test). However, at the low cyclic loading (i.e. 0.7 of the mean fracture load in the static test) this difference diminished.
- The determined damage value accumulated in the specimens showed that the difference between damage growth rate in the plain and reinforced geopolymer mortar was not significant at the lower load, however it was increased by increasing load where it was remarkably high at the load of 0.9 of the mean fracture load in the static test.
- Under the variable block loading amplitude, it was observed that the strength of the geopolymer mortar was intensively sensitive to the kind of loading amplitude. The fatigue life of specimens under the descending amplitude was significantly decreased in comparison to those under the ascending, descending-ascending and ascending-descending amplitude where not a meaning difference was observed among those.
- The reasonable agreement between experimental results and the presented model indicates that the damage curve approach might be a suitable method for approximately predicting the fatigue life of the plain and reinforced geopolymer mortar under the variable block loading amplitudes.
- Fractographic examination of the fracture surfaces of the studied geopolymer mortar revealed that the fracture mechanism is pulled out of polypropylene fibers from the geopolymer matrix. It has been concluded that the main energy absorption mechanism for retarding fatigue crack growth is the fiber pull out. Also, the multiple cracks were observed in the reinforced specimens seemingly due to the energy absorption in the fiber bridging zone.

REFERENCES

Aghazadeh Mohandesi J., Refahi A., Sadeghi Meresht E., Berenji S., 2011. Effect of temperature and particle weight fraction on mechanical and micromechanical properties sand-polyethylene terephthalate composites: A laboratory and discrete element method study. Compos Part B. 42, 1461-1467.

Akkaya Y., Peled A., Shah S.P., 2000. Parameters related to fiber length and processing in cementitious concretes. Mat Struct. 33, 515-524.

Anderson T.L., 2005. Fracture Mechanics, Fundamentals and Applications, third ed. Taylor & Francis, New York.

Banthia N., Sheng J., 1996. Fracture toughness of micro-fiber reinforced cement concretes. Cem Concr Compos. 18, 251-269.

Barbosa V.F.F., MacKenzie J.D., 2003. Synthesis and thermal behavior of potassium sialate geopolymers. Mat Let. 57, 1477-1482.

Davidovits J., 1991. Geopolymers: inorganic polymeric new materials. J Therm Anal. 37, 1633–1656.

Dias D.P., Thaumaturgo C., 2005. Fracture toughness of geopolymer concretes reinforced with basalt fibers. Cem Concr compos. 27, 49-54.

Gonzalez C., Lorca J., 2006. Multiscale modeling of fracture in fiber-reinforced concretes. Acta Materialia. 54, 4171-4181.

Kreyszig E., 2006. Advanced engineering mathematics, ninth ed. John Wiley & Sons, Singapore.

Lin T., Jia D., He P., Wang M., Liang D., 2008. Effect of fiber length on mechanical properties and fracture behavior of short carbon fiber reinforced geopolymer matrix concretes. Mat Sci Eng A. 497, 181-185.

Lin T., Jia D., He P., Wang M., 2010. In situ crack growth observation and fracture behavior of short carbon fiber reinforced Geopolymer. Mat Sci Eng A. 527, 2404-2407.

Li W., Xu J., 2009. Mechanical properties of basalt fiber reinforced geopolymeric concrete under impact loading. Mat Sci Eng A. 505(1-2), 178-186.

Manson S.S., Halford G.R., 1981. Practical implementation of the double linear damage rule and damage curve approach for testing cumulative fatigue damage. Int J Frac. 17, 169–192.

Meyers M.A., Chawla K.K., 2009. Mechanical behavior of materials, second ed. Cambridge University Press, New York.

Natali A., Manzi S., Bignozzi M.C., 2011. Novel fiber-reinforced concrete materials based on sustainable geopolymer matrix. Procedia Eng. 21, 1124-1131.

Papakonstantinou C.G., Balaguru P., Lyon R.E., 2001. Comparative study of high temperature concretes. Compos Part B. 32(8), 637-649.

Singh P.S., Bastow T., Trigg M., 2004. Outstanding problems posed by nonpolymeric particulates in the synthesis of a well-structured geopolymeric material. Cem Concr Res. 34, 1943-1947.

Singh S., Shukla A., Brown R., 2004. Pullout behavior of polypropylene fibers from cementitious matrix. Cem Concr Res. 34, 1919-1925.

Sun P., Wu H.C., 2008. Transition from brittle to ductile behavior of fly ash using PVA fibers. Cem Concr Compos. 30(1), 29-36.

Sun Z., Xu Q., 2009. Microscopic, physical and mechanical analysis of polypropylene fiber reinforced concrete. Mat Sci Eng A. 527, 198-204.

Wu S., 1982. Polymer Interface and Adhesion, first ed. Marcel Dekker, New York.

Xu H., Van Deventer J.S.J., 2000. The geopolymerisation of alumino-silicate minerals. Inl J Miner Proces. 59, 247-266.

Yunsheng Z., Wei S., Zongjin L., Xiangming Eddie Z., Chungkong C., 2008. Impact properties of geopolymer based extrudes incorporated with fly ash and PVA short fiber. Constr Buil Mat. 22, 370-383.

Zhang Y.J., Wang Y.C., Xu D.L., Li S., 2010. Mechanical performance and hydration mechanism of geopolymeric concrete reinforced by resin. Mat Sci Eng A. 527, 6574-6580.

Zhang Y., Sun W., Li Z., 2006. Impact behavior and microstructural characteristics of PVA fiber reinforced fly-ash geopolymer boards prepared by extrusion technique. J Mat Sci. 41, 2787–2794.

Zhang Z.H., Yao X., Zhu H.J., Hua S.D., Chen Y., 2009. Preparation and mechanical properties of polypropylene fiber reinforced calcined kaolin-fly ash based geopolymers. J Cent South Uni Techno. 16(1), 49–52.

Zhao Q., Nair B., Rahimian T., Balaguru P., 2007. Novel geopolymer based concretes with enhanced ductility. J Mat Sci. 42(9), 3131-3137.